

# Alternative Manoeuvres to Reduce Ship Scour

Marcella Castells-Sanabra<sup>1</sup> , Anna Mujal-Colilles<sup>1</sup>, Toni LLull<sup>2</sup>,  
Jordi Moncunill<sup>1</sup>, F.X. Martínez de Osés<sup>1</sup> , Xavi Gironella<sup>2</sup>

<sup>1</sup>(Department of Engineering and Nautical Sciences, UPC-Barcelona Tech, Barcelona, Spain)

<sup>2</sup>(Department of Civil and Environmental Engineering, UPC-Barcelona Tech, Barcelona, Spain)

(E-mail: [marcella.castells@upc.edu](mailto:marcella.castells@upc.edu))

Scouring and sedimentation effects on the seabed induced by ship propellers during ship manoeuvring near harbour structures affect both structure stability and ship manoeuvring capabilities. This contribution proposes solutions at an operational level using the automatic identification system (AIS) and a bridge simulator. Two new alternative manoeuvres were designed and tested on a bridge simulator to obtain expected maximum scour depth and the results were compared with that of real manoeuvres (i) using mooring lines, and (ii) with tug assistance. A total of 42 test scenarios combining several manoeuvres and meteorological conditions were reproduced. Results confirmed a clear reduction in erosion depth with the alternative manoeuvres, with total reduction when using the tugboat. The presented methodology can be very useful to port authorities to prevent the effects of ship erosion on harbour infrastructures.

## KEY WORDS

1. Automatic Identification System.
2. Manoeuvrability.
3. Harbour.
4. Propulsion.
5. Ship Behaviour.

Submitted: 5 November 2019. Accepted: 1 July 2020. First published online: 3 August 2020.

1. INTRODUCTION. Vessel sizes have grown rapidly over recent years to enable the transportation of larger volumes of cargo and thus reduce freight rates. This increase has resulted in more powerful ships with greater manoeuvrability and capable of higher speeds, and in time gains, but using the same old quays designed to host ships with lower draughts and less powerful propulsion systems. These rapid changes in the maritime industry are causing unexpected problems to harbour authorities. Risks associated with these larger vessels should be evaluated to establish limits on vessel dimensions and manoeuvring capabilities and thus ensure safety, efficiency and environmentally responsible use of harbour infrastructures. One of these risks is how the scouring effect on the seabed induced by ship propellers during ship arrival and departure manoeuvres near the harbour structures can affect their stability: Bergh and Magnussen (1987), Chait (1987), Fuehrer et al.

(1987) and Hamill et al. (1999, 2009) studied the propeller scouring effects using experimental scenarios; Mujal-Colilles et al. (2017a) compared previous formulas and applied them to a real case. Schokking et al. (2003), Symonds et al. (2017) and Tan and Yüksel (2018) used both numerical and experimental methods to predict propeller scouring effects. When scour occurs, the eroded material is deposited in other areas of the harbour, affecting ship manoeuvring capabilities due to a significant reduction of the water column height. Moreover, in areas of the harbour basin where the seafloor may be polluted, erosion and further resuspension of bed material can cause an important environmental problem. Permanent International Association of Navigation Congress guidelines (PIANC 2015) propose several methods to estimate propeller effects.

So far the scouring problem has been handled by harbour authorities by trying to find a structural solution and omitting existing operational solutions. However, manoeuvre patterns play an important role and, therefore, the scouring action may also be analysed from this point of view. Thus, knowledge of vessel tracks obtained through automatic identification system (AIS) data is useful to obtain daily manoeuvre patterns, traffic densities, transit duration performance and other decision support frameworks (Aarsæther and Moan, 2009; Pallotta et al., 2013; Silveira et al., 2013; Greidanus et al., 2016; Castells et al., 2017). Manoeuvre patterns obtained from AIS data can be further reproduced using a real-time full mission bridge simulator regardless of cost and time (Llull et al., 2020). Simulator studies offer accuracy and provide important information about real manoeuvres (Aarsæther and Moan, 2007). Additionally, the bridge simulator can be used to increase the number of the manoeuvring scenarios in different weather conditions.

This study uses real AIS data to analyse and further reproduce the manoeuvres that are causing or have caused an important scouring problem in harbour basins and structures. It focuses on a case study but this is a general problem that other harbours are facing and will face in the near future. A bridge simulator is used to propose new manoeuvres which minimise scour and avoid costly infrastructural solutions.

**2. CASE STUDY.** The study quay is located in the north-west Mediterranean Sea. The exact location will be kept confidential due to port authority requirements. The ship considered is a Ro-Ro ship type with a daily docking frequency at a quay with a total depth between 10 and 12 m. The ship particulars are typical values for Ro-Ro ships, with its dimensions being 199 m of length and 26 m of beam. The ship is fitted with two main engines developing 12775 kW each, two controllable pitch propellers (CPP) and two bow thrusters.

A plan view of the berthing structure and a bathymetric survey of the study area are shown in Figure 1. The berthing structure consists of a Ro-Ro berth, orientated NE, and the ship moored starboard side. The hole scoured by the main propellers of a ferry-type vessel with daily docking frequency (Llull et al., 2020) reached a total depth of 17.5 mbsl (metres below sea level), about 5–7 m deeper than the original quay seafloor. According to Mujal-Colilles et al. (2017b), a ferry-type vessel with a daily docking frequency can reach an eroding rate of up to 1.2 m in three months. The seafloor is composed of a first layer of 0.5 m in thickness and muddy and sandy sediment lying on a gravel layer of  $d_{50} = 2$  mm (2015 data provided by the port authority).

A literature review on the safety of ship berthing operations has indicated that weather and geography are common factors leading to shipping accidents (Hsu, 2015). The specific

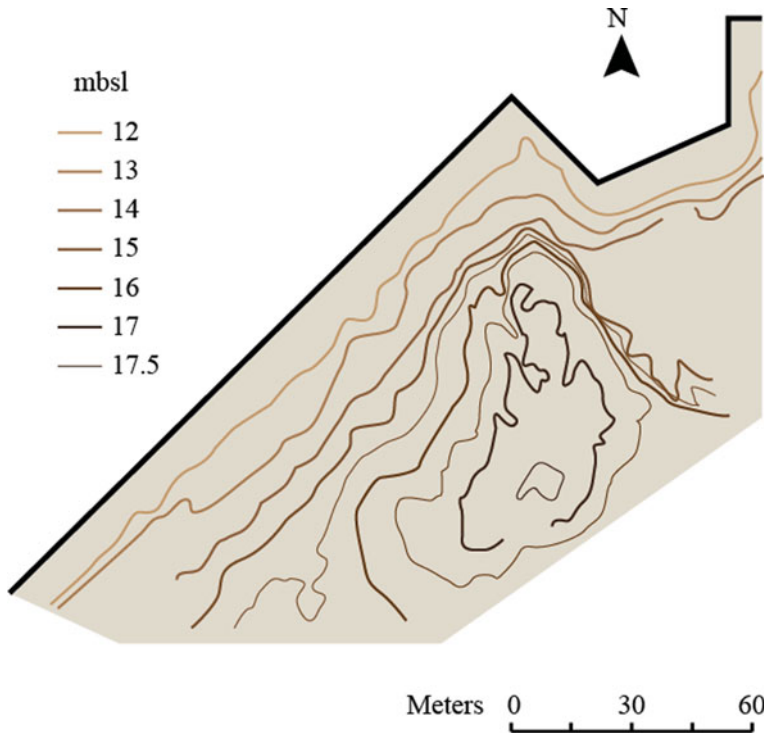


Figure 1. Bathymetry of the area of interest. Colour scale represents metres below sea level (mbsl).

meteorological conditions of the port, based on average monthly wind data, are analysed from historical data of the Spanish Meteorological Agency (AEMET). The effect of the wind on a berthing ship can be significant. It varies with wind intensity and relative direction (onshore or offshore) and ship speed and course. For instance, in strong winds it can be difficult to counteract this effect without tug assistance or the use of bow thrusters. [Figure 2](#) shows that the prevailing wind speed is force 2 in the Beaufort wind scale, the percentage of calm weather is around 24% (forces 0 and 1) and the percentage above force 5 in the Beaufort wind scale is less than 5%. The prevailing wind direction is NE (around 14%) and critical meteorological conditions in the area are NW and SW winds. Historical data show that NW events are less frequent but more intense than SW events.

Considering the NE–SW orientation of the study quay, the most harmful wind directions are, hypothetically, perpendicular and parallel to it, i.e., SE and SW winds for departure manoeuvres and NW and SW winds for arrival manoeuvres. However, as shown in [Figure 2](#), the prevailing wind direction is NE, so these winds will be considered in this study, whereas SE winds will be disregarded because their small prevalence has a lower impact on departure manoeuvres. The wind intensities used will be calm, Bf = 2 and Bf = 4, since calm and Bf = 2 are the most frequent, and Bf = 4 is the highest wind force (Bf = 5 will not be considered because it is less frequent).

3. METHODS. The methodology to study alternative manoeuvres that minimise scouring effects combines different individual methods, as detailed in [Figure 3](#). First, AIS reports

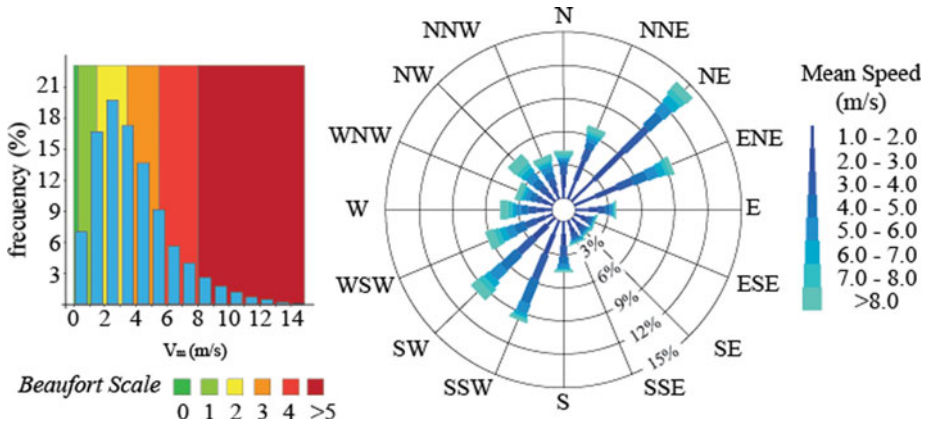


Figure 2. Mean wind speed histogram (left) in Beaufort Scale (Bf) and wind speed and direction rose plot (right) at the study port, 2012–2018 (Spanish Meteorological Agency).

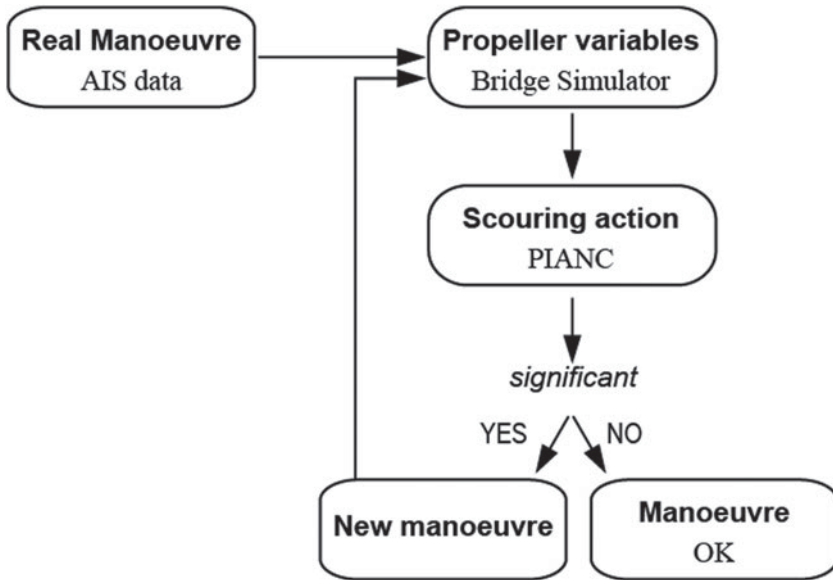


Figure 3. Combined methodology scheme.

of a real Ro-Ro ship are used to study ship manoeuvre patterns and their statistical representability. Representative arrival and departure manoeuvres at the selected harbour area are reproduced with the real-time full mission bridge simulator Transas NTPro 5000-v-5.35 and using previous AIS data to obtain scouring related propeller variables and calibrate the method with the scouring effects on the harbour basin. Thereafter, new alternative manoeuvres are designed and tested on the bridge simulator to obtain, again, expected maximum scour depth and compare the results.

3.1. *Manoeuvring pattern from AIS Data.* AIS is an automated, autonomous tracking system for ship identification and location, acting as a transponder and operating in the

Table 1. Particulars of study Ro-Ro ship and simulator ship.

Parameter	Study ship	Simulator ship
Length	199 m	182 m
Draught	6.4 m	6.5 m
Beam	26 m	25.5 m
Propulsion	12,775 kW	11,520 kW
Propellers	2 CPP	2 CPP
Propeller diameter (Dp)	5.1 m	5 m
Propeller rotating speed (n)	137 rpm	137 rpm

VHF maritime band. It is a valuable source of static and dynamic ship information and an analysis tool of harbour and open sea manoeuvres. AIS data reports were obtained from the Marine Traffic website ([marinetraffic.com](http://marinetraffic.com)) from 1 August to 30 November 2018. To identify and reproduce manoeuvre patterns, 115 (58 departure and 57 arrival) manoeuvres were analysed and the following data of each manoeuvre were extracted: coordinated universal time (UTC), position (latitude and longitude), speed over ground (SOG) and course over ground. Marine Traffic collects, decodes and presents these data in near real-time depiction with a frequency on a 60-second basis. The position to stop/start recording AIS data was (i) for departure manoeuvres, when the ship departs the port near the harbour mouth and reaches a speed of 7 knots, and (ii) for arrival manoeuvres, once the ship has passed through the harbour mouth and slows down to less than 7 knots.

Although AIS data revealed similar kinematics, there could be differences between real manoeuvres performed by different pilots/masters in terms of engine orders. Manoeuvres reproduced on the bridge simulator are always very smooth, in the sense that aggressive changes in telegraph orders are avoided. However, these aggressive changes represent a temporary, insignificant impact and will probably not affect final scour results.

**3.2. Full mission bridge simulator test.** The study ship used in the bridge simulator was chosen to be close to the real study ship, both in terms of ship particulars and propulsion system. Table 1 shows the particulars of the study ship and the simulator ship used in this research. The main differences lie in the length and engine power, with the real study ship being slightly larger. However, these differences do not affect the results substantially, as shown by Llull et al. (2018) since the propeller characteristics are similar.

A total of 42 different tests were performed by combining the following variables: manoeuvre scenario (arrival and departure), type of manoeuvre (real and alternative) and meteorological conditions, as detailed in Table 2.

Alternative manoeuvres were proposed after studying the real manoeuvres and informal surveys conducted among local experienced pilots. The requirements of these alternative manoeuvres were (i) reduce or maintain the power of main stern propellers and (ii) reduce or maintain the duration of the manoeuvres considering the weather conditions described in Table 2. Two alternative manoeuvres were proposed: (A1) without tug assistance and using mooring lines (for departure) and starting the turning circle manoeuvre before (for arrival), and (A2) with tug assistance and without using main propulsion. This second alternative manoeuvre was considered because larger ships will often require tug assistance (Hawkswood et al., 2014) and the bridge simulator used has the option to add a tug with a secondary bridge.

Table 2. Test description. Each test contains three different wind intensities [calm, 2Bf and 4Bf (Bf, Beaufort wind force scale)] and three different wind directions (NW, NE and SW).

Type of test	Scenario	Wind intensity	Wind direction
Real manoeuvre case	Arrival	Calm	–
		2 Bf and 4 Bf	NW, NE and SW
	Departure	Calm	–
Alternative manoeuvre 1, without tug assistance (A1)	Arrival	2 Bf and 4 Bf	NW, NE and SW
		Calm	–
	Departure	Calm	–
Alternative manoeuvre 2, with tug assistance (A2)	Arrival	2 Bf and 4 Bf	NW, NE and SW
		Calm	–
	Departure	Calm	–
		2 Bf and 4 Bf	NW, NE and SW

3.3. *Scouring estimation.* The propeller parameters obtained on the full mission bridge simulator were used to calculate one of the most important parameters to obtain the scouring potential, i.e., efflux velocity ( $V_0$ ), by a widely used formulation. Blaauw and van de Kaa (1978) proposed an expression based on experimental tests on scouring effects which fixes the minimum Reynolds number of the propeller and jet flow to avoid scaling effects:

$$V_0 = 1.48 \left( \frac{P}{\rho_w D_p^2} \right)^{\frac{1}{3}} \quad (1)$$

where  $P$  = engine power (W);  $\rho_w$  = density of the water ( $\text{kg}\cdot\text{m}^{-3}$ ) and  $D_p$  = diameter of the main propeller (m): see Figure 4.

The scouring action of the propeller was computed in front of a closed quay wall for non-cohesive material (Römisch and Hering, 2002) using the expression proposed by PIANC (2015):

$$1^{\text{st}} \text{ phase} \quad \frac{\varepsilon_{\max}}{d_{85}} = 0.1 C_m \left( \frac{B}{B_{cr}} \right)^{13} \quad \text{when: } 1 \leq \frac{B}{B_{cr}} \leq 1.4 \quad (2)$$

$$2^{\text{nd}} \text{ phase} \quad \frac{\varepsilon_{\max}}{d_{85}} = 4.6 C_m \left( \frac{B}{B_{cr}} \right)^{2.25} \quad \text{when: } \frac{B}{B_{cr}} \geq 1.4 \quad (3)$$

where  $\varepsilon_{\max}$  = final (or equilibrium) scour depth (m);  $B_{cr}$  = critical stability coefficient of bed material,  $\sim 1.2$ ;  $C_m = 0.3$  during berthing manoeuvres;  $d_{85}$  = diameter of bed material, 85% passing median stone diameter and  $B$  = stability coefficient. Considering that the diameter of the bed material available is  $d_{50}$  and after a sensitivity analysis showing that this variable is not key in the results,  $d_{50}$  is used.

$$B = \frac{V_{sb}}{\sqrt{d_{85} g \left( \frac{\rho_s - \rho_w}{\rho_w} - 1 \right)}} \quad (4)$$

$$\frac{V_{sb}}{V_0} = 1.9 \alpha_L \left( \frac{D_p}{L} \right) \quad (5)$$

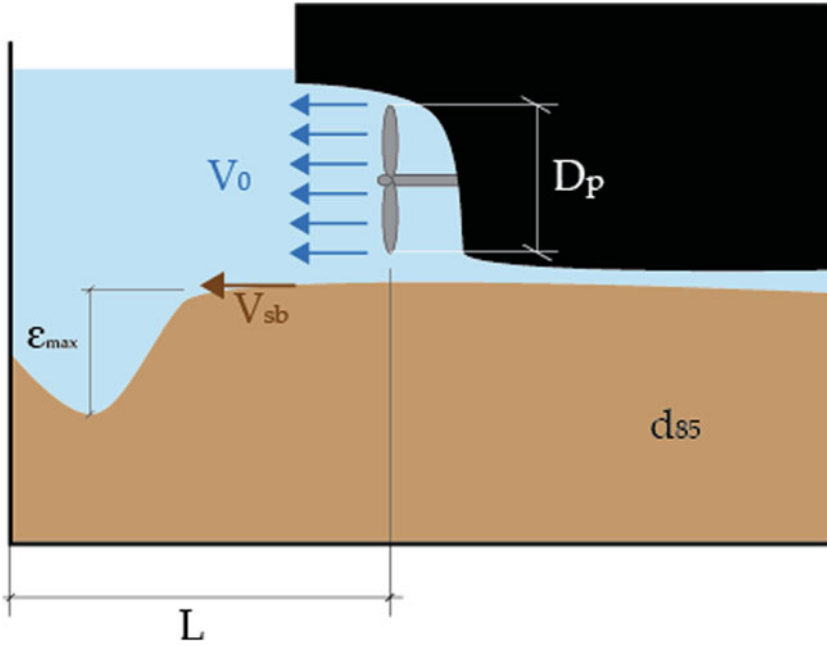


Figure 4. Sketch of the variables in Equations (1)–(5).

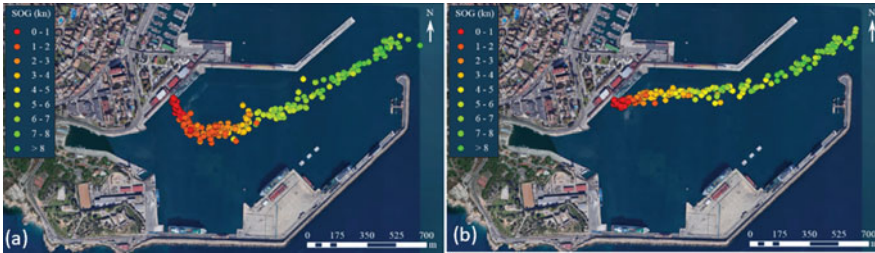


Figure 5. Ship position and speed over ground (SOG) from AIS data at case study quay from 1 August 2018 to 30 November 2018: (a) departure manoeuvres, (b) arrival manoeuvres.

where  $V_{sb}$  = flow velocity near the bed ( $m \cdot s^{-1}$ );  $g$  = gravity constant ( $m \cdot s^{-2}$ );  $\rho_s$  = density of sediment ( $kg \cdot m^{-3}$ );  $\rho_w$  = density of water ( $kg \cdot m^{-3}$ );  $\alpha_L$  = coefficient related to distance between propeller and seabed,  $\alpha_L = 1$  and  $L$  = distance between ship and quay wall (m), see Figure 4.

4. RESULTS.

4.1. AIS data. The daily manoeuvres of the study ship were analysed to identify the manoeuvre patterns over the area of interest. Figure 5 plots the arrival and departure latitude-longitude location and SOG of the AIS system.

The departure manoeuvre, Figure 5(a), consists of lateral displacement with the starboard propeller running astern and the port propeller running ahead at low regime during

the first minutes. Ship speed is 0.5 knots and the bow thruster is used intermittently to maintain a constant heading and thus compensate for torque. After 10 minutes, the propellers reverse and the ship turns to port from a heading of  $225^\circ$  to  $65^\circ$  approximately and with speed increasing from 2 to 5 knots. Finally, both propellers run parallel ahead and the ship departs the port. The approximate total duration of the departure manoeuvre is 18 minutes.

The arrival manoeuvre at the harbour basin area, [Figure 5\(b\)](#), starts with the ship turning to starboard to a heading of about  $270^\circ$  and speed reducing from 7 to 5 knots during the first 3 min. Then the ship turns to port until parallel to the quay wall, i.e., a heading of  $230^\circ$ , with both stern propellers working astern but with the port propeller regime being higher than the starboard propeller one. Now speed is below 1 knot. To begin the lateral movement towards the quayside, the starboard propeller is changed ahead while the port propeller is astern, generating a torque. The bow thruster is used during the final approach to compensate for this torque. Inertia drives the ship to the quayside. The approximate total duration of the arrival manoeuvre is 11 min.

[Figure 6](#) plots the vessel heading and position of main propellers during departure and arrival manoeuvres. As can be seen in [Figure 6](#) (right), the position of main propellers coincides with the position of the maximum bathymetry in [Figure 1](#) and shows that scour is entirely caused by the main stern propellers. This is likely due to the fact that they are bigger and have a lower clearance from the seafloor than the bow thrusters.

4.2. *Bridge simulator.* The above AIS data are necessary to mimic and reproduce the real manoeuvres on the bridge simulator. Bridge simulator results help to understand manoeuvring better and to detect critical points related to scour caused by stern propellers. The real manoeuvres were simulated for the three weather scenarios in [Table 2](#).

[Figure 7](#) shows the reproduction of the real manoeuvres on the bridge simulator in calm weather conditions.

The variable needed to estimate the scouring action during the manoeuvres is the engine power,  $P$ . However, the propeller pitch ratio,  $p'$ , and the main propeller rotation velocity,  $n$ , were also used since they help to understand the manoeuvring behaviour better. [Figure 8](#) plots the evolution of these variables during the departure manoeuvre for two different weather conditions.

The values of the propeller-related variables vary with weather conditions, being higher in worse weather conditions, see [Figure 8](#). Using the results of [Figure 8](#) as the input values in Equation (1), the efflux velocity in [Figure 9](#) is obtained as a relevant variable to predict scour depth. Tsinker (1995) and Mujal-Colilles et al. (2018a) found that the scour depth of the seabed is greater when the propeller is working ahead and the greatest cavity depth occurs in the longitudinal axis of the ship. Since the main propellers of the study ship are variable pitch propellers, the operating regime of each propeller depends on the pitch sign: (a)  $p' > 0$  the propeller is working ahead, and (b)  $p' < 0$  the propeller is working astern. This is why only efflux velocity values during forward motion are taken into account in this research.

Although the 42 tests in [Table 2](#) were reproduced and analysed on the bridge simulator, this section presents only the scenarios with potentially the most harmful wind direction: (i) SW winds (calm, 2Bf and 4Bf) for departure manoeuvres since during the first minutes it is necessary to use the port propeller in the ahead regime with more intensity, and (ii) NW winds (calm, 2Bf and 4Bf) for arrival manoeuvres since this wind direction is perpendicular to the quay and creates difficult approach conditions.

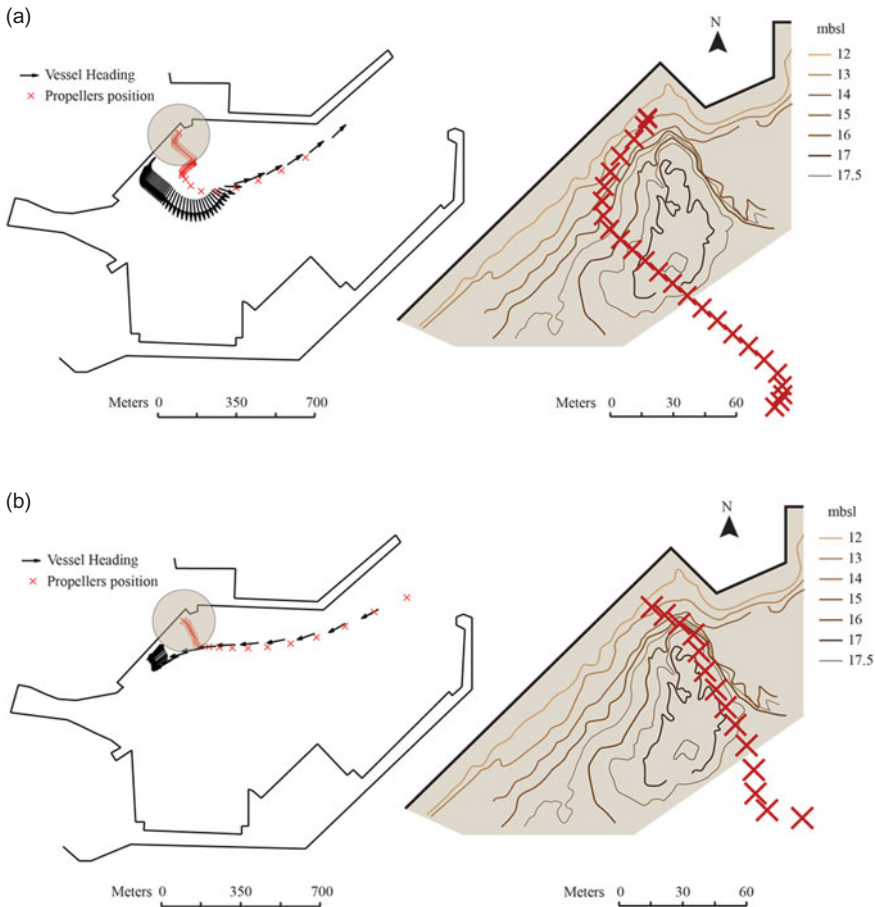


Figure 6. Ship heading and propeller position (left) and propeller position drawn on the bathymetry map (right): (a) departure manoeuvres and (b) arrival manoeuvres.

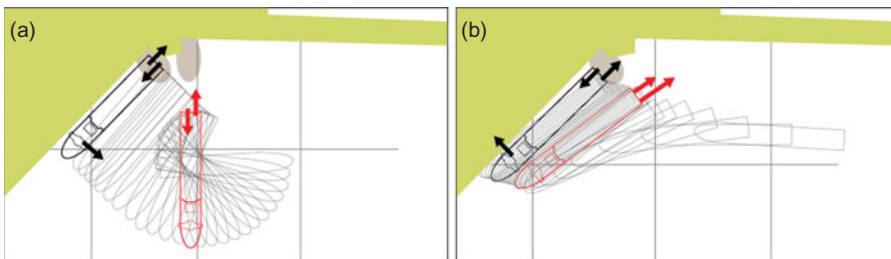


Figure 7. Bridge simulator scenarios: (a) departure manoeuvre and (b) arrival manoeuvre. Black lines represent the closest ship position to the quay; red lines represent the ship manoeuvre departing or approaching the quay.

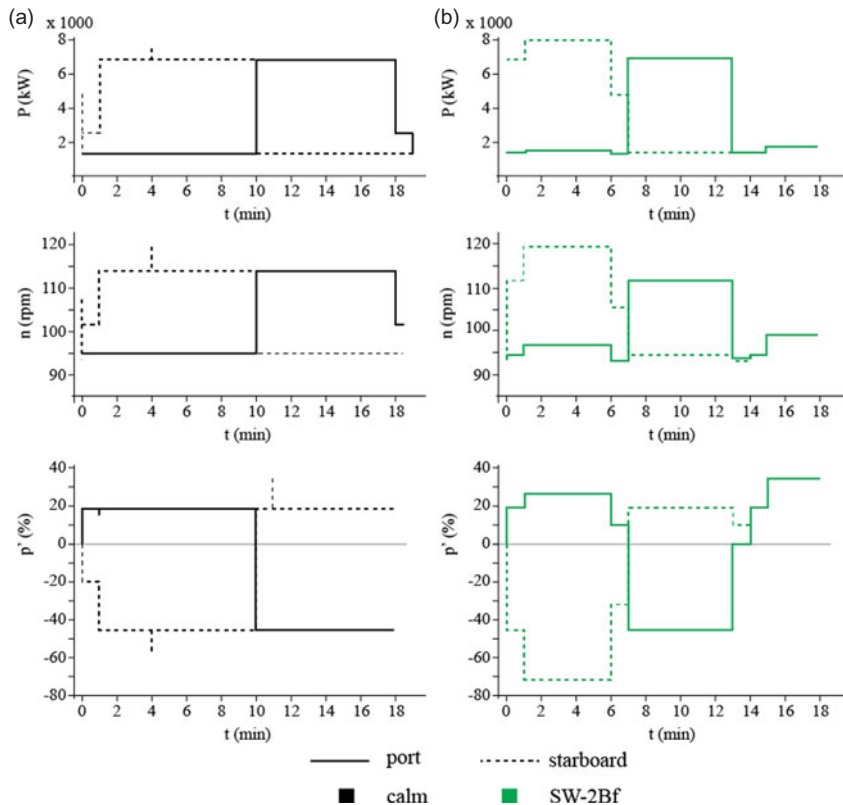


Figure 8. Time series of the propeller-related variables of the real departure manoeuvre reproduced on the bridge simulator in calm weather (black, left) and in Beaufort wind force 2 SW wind direction weather (green, right). The rpm range is 90–130 rpm. Power (top), propeller rotation velocity (middle) and propeller pitch ratio (bottom).

Figure 9 shows efflux velocity values for the departure and arrival manoeuvres considering critical wind directions. The results are quite similar but show higher values for higher wind intensity in the real departure manoeuvre due to the difficulty of holding a ship on course in bad weather.

Efflux velocity values are used to obtain the expected scour depth from Equations (2)–(5). Results for the real departure and arrival manoeuvres in the above weather conditions are shown in Figure 10.

Figure 10 shows the potential erosion for both manoeuvres considering critical wind direction. As can be observed, maximum scour only occurs at the beginning of the departure manoeuvre and at the end of the arrival manoeuvre due to the proximity of the dock wall.

5. ALTERNATIVE MANOEUVRES. After studying the real manoeuvres, alternative manoeuvres are analysed and proposed to minimise the scouring action of the main propellers. As described and documented in the sections above, the main variable responsible for scour is the use of stern propellers close to the dock wall. Therefore, scour can only be reduced by limiting the use of the main propulsion system at the beginning of the departure

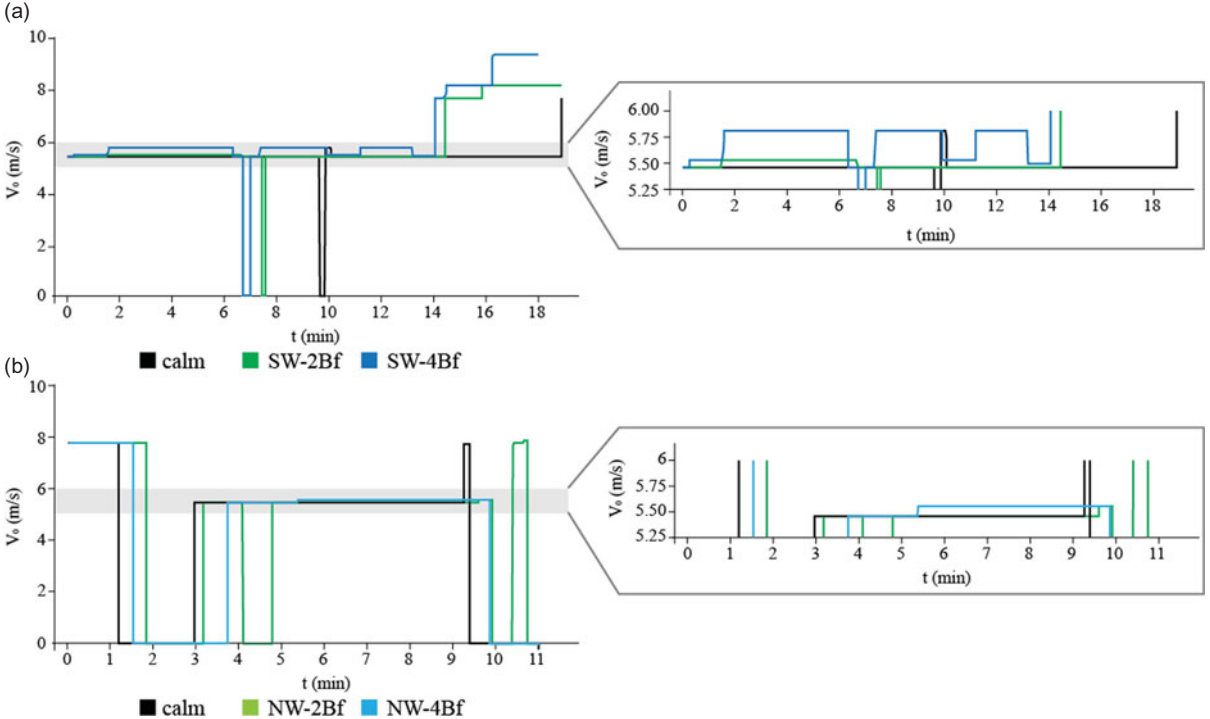


Figure 9. Efflux velocity  $V_0$ : (a) real departure manoeuvre; (b) real arrival manoeuvre. Calm (black), Beaufort wind force 2 (green) and Beaufort wind force 4 (blue).

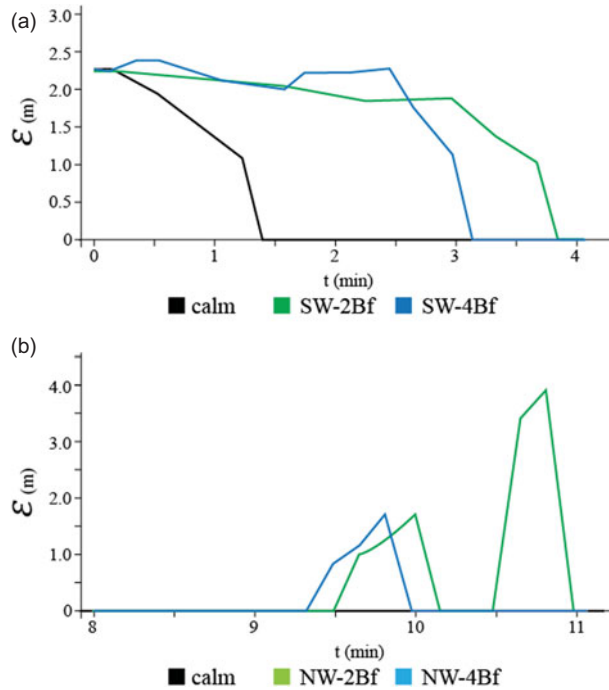


Figure 10. Potential erosion: (a) real departure; (b) real arrival. Calm (black), Beaufort wind force 2 (green) and Beaufort wind force 4 (blue).

manoeuvre and at the end of the arrival manoeuvre using either mooring lines (specifically forward spring lines) or tug assistance.

First, alternative manoeuvres without tug assistance (A1) are suggested for both departure and arrival manoeuvres. During the first minutes of the alternative departure manoeuvre, the ship is going ahead on a forward spring line (see Figure 11). By going ahead on a forward spring line, the ship's bow is pulled into the harbour and the stern swings away from the dock. After the forward spring line is released, the ship moves parallel to the quay with the help of the bow thruster. Once the ship is safely clear from the berth, the swing movement starts. The alternative arrival manoeuvre is similar to the real manoeuvre but the turning circle to starboard starts before and so the manoeuvre takes longer.

Second, alternative manoeuvres with tug assistance (A2) are proposed. The transverse force is produced by using a tug (in the aft part) and the bow thruster (in the fore part) in both manoeuvres. In the departure manoeuvre, once the ship is safely clear from the berth, the swing movement starts [Figure 12(a)]. The alternative arrival manoeuvre differs from the real manoeuvre in the final part. When the ship is just off the berth, a tug pushes the ship onto the berth from the aft port side with the help of the bow thruster [Figure 12(b)].

Following the same methodology as in the previous section, Figure 13 plots the evolution of scour assuming a levelled seafloor. The scouring action of the real and alternative manoeuvres is compared, again, only for the potentially most critical wind directions (SW for departure and NW for arrival).

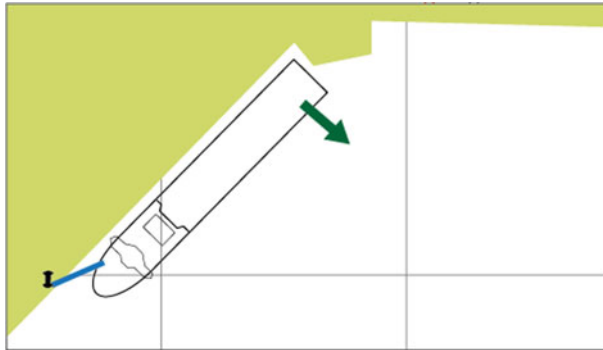


Figure 11. Alternative departure manoeuvre without tug assistance.

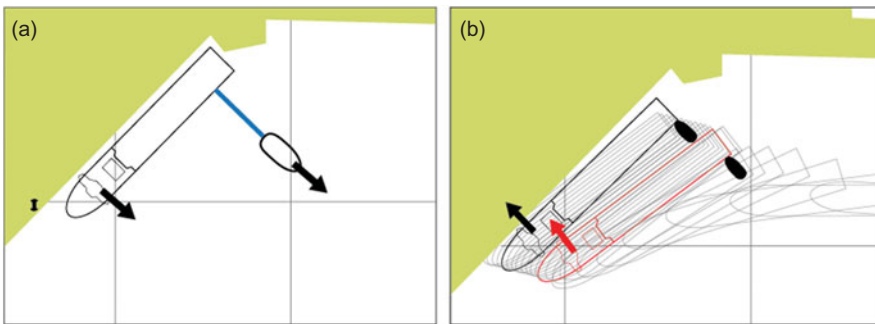


Figure 12. Alternative manoeuvres with tug assistance: (a) departure and (b) arrival.

Maximum scour results for all test cases combining all parameters in [Table 2](#) and considering other wind directions (NE for departure and arrival, NW for departure and SW for arrival) are summarised in [Figure 14](#).

As can be seen in [Figures 13](#) and [14](#), scour caused by the main propellers is reduced or, in some cases, even eliminated when using the proposed alternative manoeuvres.

6. DISCUSSION. Preliminary results obtained in the above section were considered to analyse manoeuvre behaviour. The reproduction of manoeuvres on the real-time full mission bridge simulator made it possible to know (i) the moment of the manoeuvre when scour caused by the main propellers is greatest, (ii) the influence of wind direction and intensity on manoeuvres in terms of maximum erosion depth, and (iii) the reduction in erosion obtained by using new manoeuvres.

An example of the parameters obtained from the bridge simulator for two different weather scenarios is given in [Figure 8](#). In order to maintain ship manoeuvrability and hold the ship on course in wind conditions, power requirements are slightly higher in bad weather conditions and the manoeuvre is shorter because the propellers reverse after seven minutes instead of ten. During the first minutes of the manoeuvre, more power is required for the starboard propeller running astern, and the parameters of the port propeller running ahead are higher but quite similar to those of the calm weather manoeuvre. Thus, efflux velocity and erosion depth values in [Figures 9\(a\)](#) and [10\(a\)](#) are slightly higher since only

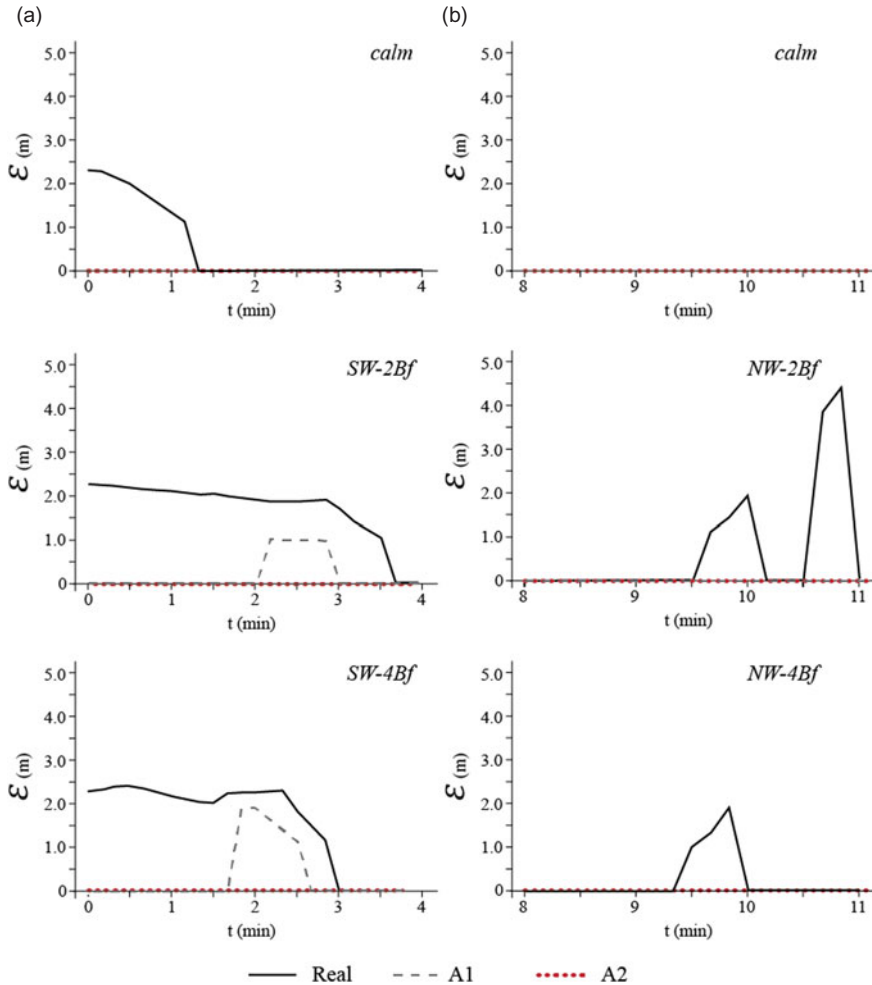


Figure 13. Expected results of scour evolution during (a) departure manoeuvre and (b) arrival manoeuvre. Black continuous line = real manoeuvre; grey dashed line = alternative manoeuvre without tug assistance (A1); red dotted line = alternative manoeuvre with tug assistance (A2).

ahead motion (port propeller) is considered and weather conditions have a small influence on the final results. Figure 10 shows that maximum scour,  $\varepsilon_{\max}$ , occurs when the operating regime of the propeller is ahead (with the propeller wash in astern direction) and near the quay. Therefore, maximum scour occurs during the first three minutes of the departure manoeuvre [Figure 10(a)] and the last minutes of the arrival manoeuvre [Figure 10(b)].

Figure 13 shows how erosion depth is reduced with the two alternative manoeuvres. The alternative departure manoeuvres without tug assistance [Figure 13(a)] lead to a decrease in the power required by the port propeller during the first three minutes, resulting in total elimination of the scouring effects in calm weather, partial reduction in prevailing weather (2Bf) and slight reduction in adverse weather (4Bf). Scour depth is totally reduced when

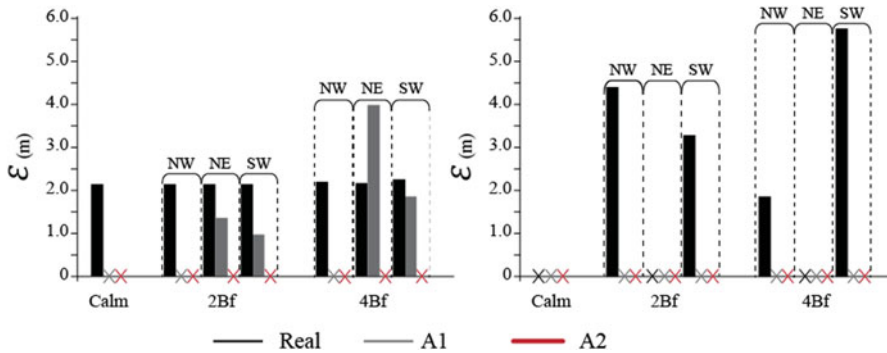


Figure 14. Maximum scour results for all test scenarios: (a) departure and (b) arrival. Black colour = real manoeuvre; grey colour = alternative manoeuvre without tug assistance (A1); red colour = alternative manoeuvre with tug assistance (A2).

tug assistance is used. As for the arrival manoeuvres [Figure 13(b)], it is observed that erosion disappears at the end of the manoeuvres.

One of the requirements of the alternative manoeuvres was to maintain or reduce the power of the main propellers. The alternative manoeuvres with tug assistance (A2) do not use main propulsion, leading to 100% reduction in power. Moreover, the main propulsion system of tugboats has a significantly smaller diameter and is located further from the seafloor, thus causing no erosion. As for the alternative manoeuvres without tug assistance (A1), the average maximum power reduction percentage is 6.5% for the departure manoeuvres. On the other hand, while the arrival manoeuvres do not result in maximum power reduction of main propellers, they take less time using this maximum power, leading to decreased scouring action. Another requirement was to reduce or at least not extend the duration of the manoeuvres. Tug assistance (A2) achieves an average time reduction of 26.4% in arrival and departure manoeuvres. Regarding the alternative manoeuvres without tug assistance (A1), the average time reduction is 29.5% for departure manoeuvres whereas most arrival manoeuvres take longer because the turning circle manoeuvre starts earlier in A1.

Finally, Figure 14 shows all 42 test scenario results. As expected, the scouring action of real manoeuvres is always more severe than that of alternative ones for all weather scenarios, especially adverse weather conditions (4Bf). However, this contribution demonstrates that the hypothetically harmful wind directions in Figure 13 are not always the worst condition for scour; the characteristics of each manoeuvre also play a crucial role in the occurrence of scour. Due to the relatively large distance between tug propellers and the seabed, and between the tug and the quay wall, Equation (5), the alternative manoeuvres with tug assistance eliminate completely the scouring effect in all weather conditions. On the other hand, the alternative manoeuvres without tug assistance reduce erosion except for the arrival manoeuvre in the worst weather (4Bf) and NE direction scenario. In this situation, the mooring line is subjected to large stresses and, when the ship is leaving the quay, it is necessary to increase the ahead regime of the port propeller to separate the ship from the quay. Weather conditions also affect the duration of manoeuvres. The alternative manoeuvres with tug assistance are always shorter than real ones, except in high wind conditions (4Bf). The alternative departure manoeuvres without tug assistance last approximately the

same as real ones, but the arrival manoeuvres are slightly longer than real ones because the manoeuvre starts prior to real one to reduce the power of the stern propellers when the ship is approaching the quay.

(Mujal-Colilles et al., 2017b) found that maximum erosion occurs in the vicinity of the quay wall. Results of this study also confirm that scour is most likely to occur near the back quay in both manoeuvres and in all weather conditions, affecting dock infrastructures. Although Figure 14 shows higher values for arrival manoeuvres, the duration of their scouring action is shorter (less than one minute) compared with the departure manoeuvres (three minutes approximately), with the latter therefore posing the most damaging scenarios. These findings are in agreement with the experimental results of Mujal-Colilles et al. (2018b).

PIANC guidelines are used to calculate the maximum scour depth on the study quay. However, there is a lack of formulation to evaluate the potential scouring action of main propellers in a confined area. For this reason, (PIANC, 2015) proposes a set of equations extracted from Römisch and Hering (2002) to calculate scour caused by confined washes, but bearing in mind that their use is mainly recommended for transverse thrusters.

Although shallow water and bank effects have an influence on ship behaviour and the full mission bridge simulator should be able to reproduce them, these factors are not considered in this research due to slow ship speed during arrival and departure manoeuvres (PIANC, 1980). Moreover, the expected tugboat scouring action during the alternative manoeuvres has not been included either for two reasons. First, the potential scour would occur in a different location: (i) during the arrival manoeuvre wash generated by the tug is directed outwards, perpendicular to the ship's heading, away from the quay wall to the outer basin, and (ii) during the departure manoeuvre, the tug is farther from the quay than the vessel, which is situated between the tug and the berth side, acting as a disturbing element for the free jet flow expansion. Second, the larger distance from the tug propeller to the wall and to the bottom (compared with that of the vessel) and its smaller dimensions indicate a low scouring action by applying the formulation [Equations (2)–(5)] since they rely mainly on these parameters.

**7. CONCLUSION.** The AIS and the bridge simulator are useful tools to obtain parameters that otherwise are difficult to estimate when determining the potential scouring action of a ship. These parameters are used to calculate propeller velocities, which in turn are used to calculate maximum scour and to identify potentially affected areas. It is found that greatest scour occurs near the back quay wall, when the stern propellers are working ahead, affecting harbour infrastructures, mainly during the departure manoeuvre. Weather conditions also have an influence on manoeuvres, especially during arrival.

A qualitative method to reduce or even prevent scour using alternative manoeuvres for a study-case ship and a specific harbour area is presented. The results confirm a clear reduction of erosion depth. First, alternative manoeuvres without tug assistance are proposed. However, manoeuvres using a forward spring line have some limitations in adverse weather conditions (4Bf). Moreover, mooring lines for bigger ships are subjected to large stresses which may exceed a safe working load, thus putting the ship in danger and compromising the resistance of bollards against impact loads. Reduction of erosion and time is even

more significant for alternative manoeuvres with tug assistance regardless weather conditions. Specifically, in departure manoeuvres the stern propellers do not work until the swing movement begins, away from the quay. However, this second option has an economic cost for ship owners which should be evaluated before proposing it as a solution for harbour infrastructures.

Therefore, AIS and the bridge simulator provide data that can be transformed into meaningful information for operational decision support to reduce the impact of erosion and sedimentation resulting from ship manoeuvres and used to assess port infrastructure and help port authorities and ship masters. Although the solution proposed in this contribution is for a specific port and ship, it can be used qualitatively in other scenarios. However, a quantitative data analysis should be carried out in order to find general assumptions for all ports, ship types and weather conditions.

### ACKNOWLEDGEMENTS

The authors greatly acknowledge the contribution of Guillermo Pedrosa Eguílaz from Barcelona School of Nautical Studies (UPC).

### FINANCIAL SUPPORT

This research has been supported by MINECO (Ministerio de Economía y Competitividad) and FEDER (Unión Europea-Fondo Europeo de Desarrollo Regional 'Una Manera de Hacer Europa') from the Spanish Government through project BIA2012-38676-C03-01 and TRA2015-70473-R.

### REFERENCES

- Aarsæther, K. G. and Moan, T. (2007). Combined maneuvering analysis, AIS and full-mission simulation. *TransNav?: International Journal on Marine Navigation and Safety of Sea Transportation*, **1**, 31–36.
- Aarsæther, K. G. and Moan, T. (2009). Estimating navigation patterns from AIS. *Journal of Navigation*, **62**(04), 587. doi:10.1017/S0373463309990129
- Bergh, H. and Magnussen, N. (1987). Propeller erosion and protection methods used in ferry terminals in the port of Stockholm. *Bulletin of the Permanent International Association of Navigation Congress (PIANC)*, **58**, 112–120.
- Blaauw, H. G. and van de Kaa, E. J. (1978). Erosion of Bottom and Sloping Banks Caused by the Screw Race of Manoeuvring Ships, 7th International Harbour Congress, Antwerp, Belgium. Publication No. 202, pp. 1–12. Delft Hydraulics Lab, Netherlands.
- Castells, M., Martínez, F. J., Martín, A., Mujal-Colilles, A. and Gironella, X. (2017). Tools for Evaluation Quay Toe Scouring Induced by Vessel Propellers in Harbour Basins During the Docking and Undocking Manoeuvring. *Safety of Sea Transportation: Proceedings of the 12th International Conference on Marine Navigation and Safety of Sea Transportation (TransNav 2017)*, June 21–23, 2017, Gdynia, Poland. CRC Press, The Netherlands, pp. 61–66. doi:10.1201/9781315099088-10.
- Chait, S. (1987). Undermining of quaywalls at South African ports due to the use of bow thrusters and other propeller units. *Bulletin of the Permanent International Association of Navigation Congress (PIANC)*, **58**, 107–110.
- Fuehrer, M., Pohl, H. and Römish, K. (1987). Propeller jet erosion and stability criteria for bottom protections of various constructions. *Bulletin of the Permanent International Association of Navigation Congress (PIANC)*, **58**.
- Greidanus, H., Alvarez, M., Eriksen, T. and Gammieri, V. (2016). Completeness and accuracy of a wide-area maritime situational picture based on automatic ship reporting systems. *Journal of Navigation*, **69**(1), 156–168. doi:10.1017/S0373463315000582.
- Hamill, G., Johnston, H. T. and Stewart, D. (1999). Propeller wash scour near quay walls. *Journal of Waterway, Port, Coastal and Ocean Engineering*, **125**(4), 170–175.

- Hamill, G., Ryan, D. and Johnston, H. T. (2009). Effect of rudder angle on propeller wash velocities at a seabed. *Proceedings of the Institution of Civil Engineers-Maritime Engineering*, **162**(1), 27–38.
- Hawkswood, M. G., Lafeber, F. H. and Hawkswood, G. M. (2014). Berth scour protection for modern vessels. In PIANC World Congress, San Francisco, USA, 2014.
- Hsu, W. K. K. (2015). Assessing the safety factors of ship berthing operations. *Journal of Navigation*, **68**(3), 576–588. doi:10.1017/S0373463314000861
- Llull, T., Mujal-Colilles, A., Castells-Sanabra, M., Gironella, X., Martinez, F. J., Martin, A. and Sanchez-arcilla, A. (2018). Hybrid Tool to Prevent Ship Propeller Erosion. In Proceedings of the ASME 2018 37th International Conference on Ocean, Offshore and Arctic Engineering (OMAE2018), June 17–22, 2018, Madrid, Spain. American Society of Mechanical Engineers (ASME), Vol. 4, 1–10.
- Llull, T., Mujal-Colilles, A., Castells-Sanabra, M. and Gironella, X. (2020). Composite methodology to prevent ship propeller erosion. *Ocean Engineering*, **195**, 106751. doi:10.1016/j.oceaneng.2019.106751.
- Mujal-Colilles, A., Gironella, X., Sanchez-Arcilla, A., Puig-Polo, C. and Garcia, M. (2017a). Erosion caused by propeller jets in a low energy harbour basin. *Journal of Hydraulic Research*, **55**(1), 121–128. doi:10.1080/00221686.2016.1252801.
- Mujal-Colilles, A., Gironella, X., Sanchez-Arcilla, A., Puig-Polo, C. and Garcia, M. (2017b). Study of the bed velocity induced by twin propellers. *Journal of Waterway, Port, Coastal, and Ocean Engineering*, **143**(5), 04017013. doi:10.1061/(ASCE)WW.1943-5460.0000382.
- Mujal-Colilles, A., Llull, A., Castells, M., Gironella, X., Martinez, F. J. and Sanchez-Arcilla, A. (2018a). Ship manoeuvring effects on propeller induced erosion. In International Conference on the Application of Physical Modelling to Port and Coastal Protection, pp. 1–7. Available at: <http://hdl.handle.net/2117/118488>.
- Mujal-Colilles, A., Castells-Sanabra, M., Llull, T., Gironella, X. and Martinez, F. J. (2018b). Stern twin-propeller effects on harbor. *Water*, **10**(w), doi:10.3390/w10111571.
- Pallotta, G., Vespe, M. and Bryan, K. (2013). Vessel pattern knowledge discovery from AIS data: A framework for anomaly detection and route prediction. *Entropy*, **15**(12), 2218–2245. doi:10.3390/e15062218.
- PIANC. (1980). Permanent International Association of Navigation Congresses, Optimal Lay-Out and Dimensions for the Adjustment to Large Ships of Maritime Fairways in Shallow Seas, Straits and Maritime Waterways. International Commission for the Reception of Large Ships, Brussels, Belgium.
- PIANC. (2015). Permanent International Association of Navigation Congresses, Guidelines for Protecting Berthing Structures from Scour Caused by Ships. Report no. 180. The World Association for Waterborne Transportation Infrastructure, Brussels, Belgium.
- Römisch, K. and Hering, W. (2002). Input data of propeller induced velocities for dimensioning of bed protection near quay walls. *Bulletin of the Permanent International Association of Navigation Congresses*, **109**, 5–11.
- Schokking, L. A., Janssen, P. C. and Verhagen, H. J. (2003). Bowthruster-induced damage. *Bulletin of the Permanent International Association of Navigation Congress (PIANC)*, 114, 53–63.
- Silveira, P. A. M., Teixeira, A. P. and Soares, C. G. (2013). Use of AIS data to characterise marine traffic patterns and ship collision risk off the coast of Portugal. *Journal of Navigation*, **66**(6), 879–898. doi:10.1017/S0373463313000519.
- Symonds, A., Britton, G., Donald, J. and Loehr, H. (2017). Predicting propeller wash and bed disturbance by recreational vessels at marinas. *Bulletin of the Permanent International Association of Navigation Congress PIANC 2016 Yearbook*, 70–80. Available at: <https://www.pianc.org/uploads/files/Yearbook/Yearbook-2016/Technical-Articles.pdf>.
- Tan, R. Y. and Yüksel, Y. (2018). Seabed scour induced by a propeller jet. *Ocean Engineering*, **160**, 132–142. doi:10.1016/J.OCEANENG.2018.04.076.
- Tsinker, G. P. (1995). *Marine Structures Engineering: Specialized Applications*. Boston, MA: Springer US. doi:10.1007/978-1-4615-2081-8.